Duality-Free Decomposition Based Data-Driven Stochastic Security-Constrained Unit Commitment

Ding, Tao; Yang, Qingrun; Liu, Xiyuan; Huang, Can; Yang, Yongheng; Wang, Min; Blaabjerg, Frede

Published in:
I E E E Transactions on Sustainable Energy

DOI (link to publication from Publisher):
10.1109/TSTE.2018.2825361

Publication date:
2019

Document Version
Accepted author manuscript, peer reviewed version

This article has been accepted for publication in a future issue of this journal, but has not been fully edited. Content may change prior to final publication. Citation information: DOI 10.1109/TSTE.2018.2825361, IEEE Transactions on Sustainable Energy

Duality-Free Decomposition Based Data-Driven Stochastic Security-Constrained Unit Commitment

Tao Ding, *Member, IEEE*, Qingrun Yang, *Student Member, IEEE*, Xiyuan Liu, *Student Member, IEEE*, Can Huang, *Member, IEEE*, Yongheng Yang, *Senior Member, IEEE*, Min Wang, Frede Blaabjerg, *Fellow, IEEE*

***Abstract*— To incorporate the superiority of both stochastic and robust approaches, a data-driven stochastic optimization is employed to solve the security-constrained unit commitment model. This approach makes the most use of the historical data to generate a set of possible probability distributions for wind power outputs and then it optimizes the unit commitment under the worst-case probability distribution. However, this model suffers from huge computational burden, as a large number of scenarios are considered. To tackle this issue, a duality-free decomposition method is proposed in this paper. This approach does not require doing duality, which can save a large set of dual variables and constraints, and therefore reduces the computational burden. In addition, the inner max-min problem has a special mathematical structure, where the scenarios have the similar constraint. Thus, the max-min problem can be decomposed into independent sub-problems to be solved in parallel, which further improves the computational efficiency. A numerical study on an IEEE 118-bus system with practical data of a wind power system has demonstrated the effectiveness of the proposal.**

***Index Terms*—Data-driven stochastic optimization; duality-free decomposition; security-constrained unit commitment; distributionally robust optimization**

Nomenclature

$t \in \mathcal{T}$	Hourly periods, running from 1 to $T=\lvert\mathcal{T}\rvert$.
$l \in \mathcal{L}$	Transmission lines, running from 1 to $L=\lvert\mathcal{L}\rvert$.
$b \in \mathcal{B}$	Buses, running from 1 to $B=\lvert\mathcal{B}\rvert$.
$q \in \mathcal{Q}$	Wind units, running from 1 to $Q=\lvert\mathcal{Q}\rvert$.
$g \in \mathcal{G}$	Thermal units, running from 1 to $G=\lvert\mathcal{G}\rvert$.
$\omega \in \Omega$	Wind power scenarios, running from 1 to $N=\lvert\Omega\rvert$.
$s \in \mathcal{S}_g$	Startup segments, running from 1 (hottest) to $S_g=\lvert\mathcal{S}_g\rvert$ (coldest).
Ψ	Confidence set for uncertain probability distribution of wind power.
$\mathbf{f}(b), \mathbf{t}(b)$	Transmission lines subset starting from bus b or ending at bus b.
$\mathbf{G}(b), \mathbf{W}(b)$	Thermal or wind units subset located at bus b.
$P_{gt\omega}$	Power output of thermal unit g at period t under scenario ω [MW].
$W_{qt\omega}$	Forecasted power output of wind unit q at period t under scenario ω [MW].
$L_{bt\omega}^{\text{shed}}$	Load shedding imposed on bus b at period t under scenario ω [MW].
$PL_{lt\omega}$	Power flow on transmission line l at period t under scenario ω [MW].
$\theta_{at\omega}, \theta_{bt\omega}$	Phase angle of bus a and bus b at period t under scenario ω [rad].
$r_{gt\omega}$	Spinning reserve provided by thermal unit g at period t under scenario ω [MW].
u_{gt}	Commitment status that is equal to 1 if thermal unit g is online at period t.
v_{gt}	Startup status that is equal to 1 if thermal unit g starts up at period t.
z_{gt}	Shutdown status that is equal to 1 if thermal unit g shuts down at period t.
δ_{gst}	Startup type s of thermal unit g, which is equal to 1 at the period t where the unit starts up and has been offline within $[T_{gs}^{SU}, T_{g,s+1}^{SU})$ hours.
π_ω	Probability of wind power scenario ω.
π_ω^0	Probability of wind power scenario ω from data
$C_g^{\text{NL}}, C_g^{\text{SD}}$	No-load cost and shutdown cost of thermal unit g [$].
C^{LOL}	Load shedding cost [$/MWh].
C_{gs}^{SU}	Startup cost of thermal unit g when the unit starts up and has been offline within $[T_{gs}^{SU}, T_{g,s+1}^{SU})$ hours [$].
L_{bt}	Load demand located at bus b at period t [MW].
$PL_l^{\max}$	Capacity of transmission line l [MW].
x_{ab}	Reactance of transmission line from bus a to bus b [per unit].
R_t	Spinning reserve requirement at period t [MW].
TU_g, TD_g	Minimum uptime and minimum downtime of thermal unit g [h].
$P_g^{\max}, P_g^{\min}$	Maximum and minimum power output of thermal unit g [MW].
SU_g, SD_g	Startup capability and shutdown capability of thermal unit g [MW].
RU_g, RD_g	Ramp-up rate and ramp-down rate of thermal

This work was supported in part by National Key Research and Development Program of China (2016YFB0901900), in part by National Natural Science Foundation of China (Grant 51607137), in part by China Postdoctoral Science Foundation (2017T100748), in part by the project of State Key Laboratory of Electrical Insulation and in part by Power Equipment in Xi'an Jiaotong University (EIPE16301). This work was performed under the auspices of the U.S. Department of Energy by Lawrence Livermore National Laboratory under Contract DE-AC52-07NA27344 with Release Number LLNL-JRNL-TBD.

T. Ding, Q. Yang and X. Liu are with the State Key Laboratory of Electrical Insulation and Power Equipment, Department of Electrical Engineering, Xi'an Jiaotong University, Xi'an, Shaanxi, 710049, China;

C. Huang is with the Lawrence Livermore National Laboratory, Livermore, CA, USA.

Y. Yang and F. Blaabjerg are with the Department of Energy Technology, Aalborg University, Aalborg DK-9220, Denmark.

M. Wang is with the Shaanxi Electric Power Corporation Economic Research Institute, Xi'an, Shaanxi, 710075, China.

This article has been accepted for publication in a future issue of this journal, but has not been fully edited. Content may change prior to final publication. Citation information: DOI 10.1109/TSTE.2018.2825361, IEEE Transactions on Sustainable Energy

unit g [MW/h].

α Pre-designed confidence level.

β Controllable parameter for confidence set.

N_s The Number of scenarios.

K The Number of historical data.

I. INTRODUCTION

Security constrained unit commitment (SCUC) is one of the important functions for scheduling generators in day-ahead power system operation [1]-[3]. It determines the on/off status of all dispatchable units over a given number of horizons while satisfying all the physical constraints of generators and the power network. However, with a high penetration of wind power into the power grid, many challenging issues arise [4]. The wind power output is highly stochastic and volatile, which hinders their efficient and secure large-scale deployment and challenges the SCUC of power systems. Thus, the uncertainty of the wind power output should be considered in the SCUC scheduling problem. With this, many studies have been done in the literature [5-21]. They can be categorized into three groups: 1) interval constrained unit commitment (ISCUC) [5-6], 2) stochastic security-constrained unit commitment (SSCUC) [7-14], and 3) robust security-constrained unit commitment (RSCUC) [15-21].

SSCUC models generate several wind power scenarios associated with various probabilities to describe uncertainties. These models minimize the expected total cost while satisfying all operational constraints under all the scenarios [7]. In contrast, the RSCUC models are immune against the wind power uncertainties within a predefined uncertainty set [15]. These models essentially minimize the total cost under the worst-case scenario. The computational burden of the RSCUC models mainly depends on the definition of their uncertainty sets [20]. It should be noted that both the SSCUC and RSCUC models can be cast as a two-stage optimization problem. The first-stage decisions find the optimal unit commitment that cannot be changed once they are optimized before the true wind power realization; the second-stage decisions are adjusted to the realization of the wind power generation, which provides the recourse for the system. The difference of the two models is that the RSCUC expects to find the solution that can fully guarantee the feasibility for any possible realization within the uncertainty set, while the SSCUC only protects the system under the selected scenarios.

Nevertheless, compared with the SSCUC models, the RSCUC models may give relatively conservative solutions. Recently, the concept of uncertainty budget has been proposed to reduce over-conservative decisions. Several methods to construct the proper uncertainty sets based on historical data were introduced in [22] to reduce the conservativeness while maintaining the robustness of the solutions. In addition, [23] introduced a risk-constrained robust unit commitment model, where the uncertainty set was divided into several probability-blocks with respect to the data sets. A multistage adaptive robust unit commitment model was set up in [24], where dynamic uncertainty sets were utilized to capture the temporal and spatial correlations of renewable energy as well as the sequential nature of the dispatch process. Furthermore, a two-stage min-max regret robust unit commitment was established in [25] to reduce the conservativeness, where the maximum regret in the robust optimization framework was considered. Moreover, adjustable uncertainty sets according to different system-risk levels were adopted to achieve the operational flexibility for day-head unit commitment [26]. Then, a novel unified stochastic and robust unit commitment model was proposed in [27] to reduce the expected cost by adjusting the weights in the objective function.

Compared with the RSCUC models, although the SSCUC models can avoid the conservative total cost, the system security cannot be sufficiently guaranteed. Therefore, many efforts were devoted into the chance-constrained security-constrained unit commitment (CSCUC) [28-30]. The CSCUC model ensures the feasibility for the constraints with stochastic variables in a certain probability. Since the chance constraints generally lead to the non-convexity, the CSCUC problem is usually solved by means of a sample-average approximation approach [28]. Only certain CSCUC models can be equivalently transformed into deterministic SCUC models [29], which leads to the notion of risk-averse SCUC models that include the operational risk. In general, the risk exposure of the power system is considered in the objective function or in the constraints of the SCUC model. Typically, the considered risk includes the loss-of-load and the wind curtailment [30]. The risk-averse SCUC model allows a tradeoff between the expected dispatch costs and the operational risks caused by uncertainties [31]. Recently, several risk measures have been applied to SCUC models, such as the mean-variance [32], shortfall probability [33], and conditional value-at-risk (CVaR) [31, 34].

Generally, stochastic programming methods cannot cover all possible realizations of uncertainties. A particular probability distribution of random parameters is usually assumed, which may be biased in practice. Although the robust optimization can take all realizations into consideration and protect the system against a pre-defined uncertainty set, it gives a more conservative solution than the stochastic approach. The chance-constrained framework is usually reformulated as a large-scale mixed integer programming model, depending on the number of scenarios considered in the model, which increases the computational burden. Also, as one of the stochastic approaches, it shares the same disadvantages with the SUC—it is not possible to enumerate all the scenarios and the solution depends on the assumed distribution in the model.

To achieve a more reasonable unit commitment with the superiority of stochastic and robust optimization models, the data-driven framework can be adopted to find a more suitable solution. It should be robust but less conservative. Based on the historical data, a series of possible probability distribution of wind power can be constructed. This model takes advantage of data information and considers the worst-case distribution of the uncertainties. When comparing with the case considering the worst-case scenario in the robust optimization approach, the

This article has been accepted for publication in a future issue of this journal, but has not been fully edited. Content may change prior to final publication. Citation information: DOI 10.1109/TSTE.2018.2825361, IEEE Transactions on Sustainable Energy

data-driven model yields less conservativeness. It aims to find an optimal solution under the worst probability distribution, known as “distributionally robust optimization” or “data-driven optimization” [35]-[38]. Recently, this approach is also used to solve the UC problem [39], [40]. More importantly, it does not require probabilistic distribution assumption. Instead, it allows an ambiguous distribution within the confidence set. This leads to a more robust solution compared with the stochastic optimization.

However, the model in [39] has difficulties in solving large-scale problems. More specifically, due to the “max-min” duality, it is difficult to find the worst-case scenario. Clearly, a larger number of scenarios will lead to a more precise optimal solution, while increasing the complexity and computational burden. In that case, the problem becomes intractable or even unsolvable. In the prior-art work, the decomposition method has been proposed to tackle this issue [41], [42]. For instance, in [41], the augmented Lagrangian relaxation method was employed to decompose the large-scale problem into several small sub-problems (one for each scenario). However, this is only applicable to single-level stochastic programming models. In this paper, the proposed data-driven distributionally robust optimization is essentially a “min-max-min” tri-level model to efficiently solve the above issues. To our best knowledge, how to decompose the tri-level optimization model has not been addressed yet in the literature.

The main contributions of this paper are summarized as:

(i) A data-driven stochastic SCUC model is set up using the practical data that incorporates the superiority of stochastic and robust optimization models. Meanwhile, the practical wind speed is analyzed under four seasons during one year, which facilitates the stochastic SCUC model.

(ii) A novel decomposition approach is proposed to solve the tri-level data-driven stochastic unit commitment model. This approach does not require dualization, which can save a large set of dual variables and constraints and thus reduce the computational burden. Additionally, due to its special structure, the inner max-min problem can be decomposed into independent sub-problems and then solved in parallel, which further improves the computational efficiency.

The rest of the paper is organized as follows: Section II investigates the modeling of wind power generation scenarios. In Section III, a data-driven stochastic security-constrained unit commitment (SCUCU) model is set up considering the uncertain probability distribution of wind power. A duality-free based Bender’s decomposition algorithm is then proposed to solve the data-driven stochastic SCUC model in Section IV. In Section V, numerical results and comparisons on a standard IEEE 118-bus system demonstrate the effectiveness of the proposed model and method. Finally, conclusions are drawn in Section VI.

II. Wind Power Scenario Generation

Wind power generation scenarios are usually generated with Monte Carlo simulations using a predefined wind power distribution. However, in order to describe a precise wind power distribution, wind speed characteristics should be analyzed according to the wind farm historical data. In this paper, the wind speed is characterized by four seasons in a year. Taking one real-field wind farm in China as an example, where the wind speed data in the past 10 years is utilized:

Fig. 1 depicts the wind speed in one day (24 hours) and one month (720 hours). It can be observed that the wind speed is stochastic and volatile. However, the wind speed is relatively periodic and the daily wind speed distribution over a long period is similar.

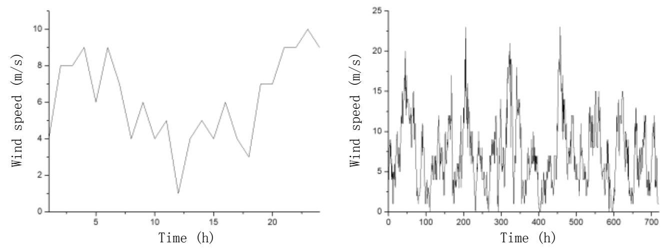

(a) (b)

Fig. 1. Wind speed distribution in the wind farm located in Northwest China for: (a) one day and (b) one month.

For one day, Fig. 2 shows the wind speed distribution at 00:00 AM and 12:00 PM. It can be observed that the wind speed distribution has a “double-peak” nature, where the peak values are near 0 m/s and 5 m/s, respectively. The number of scenarios becomes smaller with the increase in wind speed. Meanwhile, a comparison of Fig. 2(a) and (b) implies that the average wind speed at 12:00 PM is higher than that at 00:00 AM. Moreover, the number of scenarios with high wind speeds (more than 18 m/s) is larger at 12:00 PM than that at 00:00 AM. As a result, the wind speed modeling should consider the daily time-series characteristics.

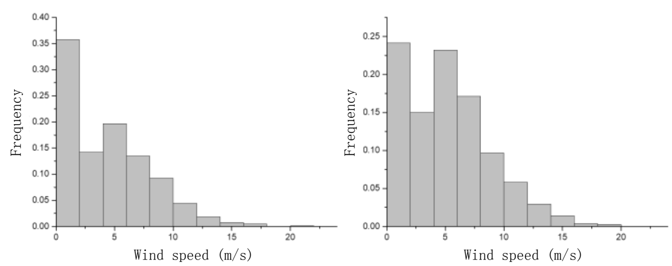

(a) (b)

Fig. 2. Wind speed distribution of the wind farm in one day at: (a) 00:00 AM and (b) 12:00 PM.

However, for one year, Fig. 3 depicts the distribution of wind speeds, which shows that the high wind speed condition is more frequent in spring and winter than that in summer and autumn. In spring, the peak wind speed is around 7.5 m/s and there are several scenarios with the wind speed higher than 12.5 m/s; in summer, the peak is around 5 m/s and the number of scenarios with the wind speed higher than 10 m/s is small. The statistics from historical data suggest that four seasons have different wind speed characteristics. As a consequence, daily time-series characteristics should be modeled separately.

Based on the historical data, the daily wind power density can be estimated through various prior-art probabilistic forecast approaches. Meanwhile, in [43], a method that can generate statistical scenarios of the wind power generation considering spatial-temporal interdependence was introduced, and it is also used in this paper. Then, 1000 wind power scenarios are set up at the beginning according to the estimated probability density function describing the uncertainty in forecasts. Furthermore, the scenario generation technique is based on building joint predictive densities from the marginal ones. The interdependent structure of wind power generation through time and space is modeled by the covariance matrix of the multivariate Gaussian distribution. Finally, it is known that a large number of scenarios are required to fully characterize the wind power uncertainty. However, increasing the number of scenarios makes the stochastic SCUC modelling become computationally intractable. To retain the tractability and maintain the statistical information, the probability distance-based scenario-reduction technique [44] is employed in this paper.

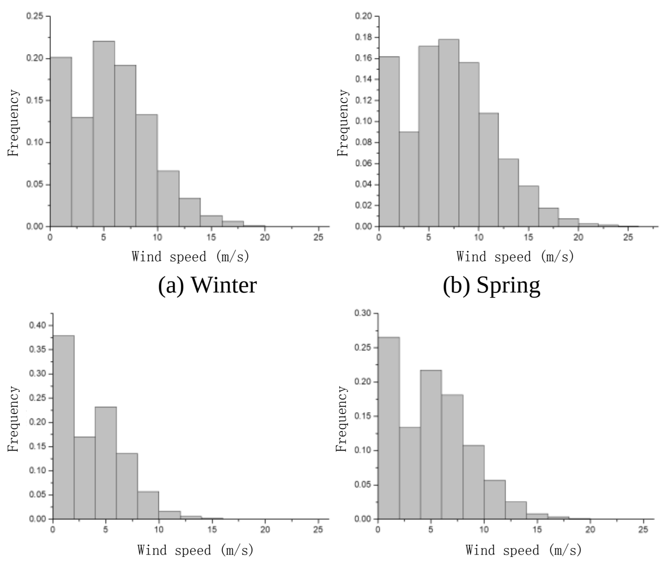

Fig. 3. Wind speed distribution of the wind farm in a year.

III. Data-Driven Stochastic SCUC Model

A. General Stochastic SCUC Model

In this section, the general stochastic SCUC model is set up in a tight and compact MILP formulation [39]. It was discussed in [39] that the tight and compact formulation could improve the computational efficiency of stochastic UC models, since a smaller searching space and a faster searching process for the branch-and-cut algorithm are enabled.

The stochastic SCUC optimization problem aims to minimize the expected operational cost over a given number of time horizons while satisfying various physical constraints. Specifically, the objective function should include: (i) the fixed production cost; (ii) startup cost; (iii) shutdown cost; (iv) production cost; and (v) loss-of-load cost, such that

$$\min \sum_{t\in\mathcal{T}}\sum_{g\in\mathcal{G}}\left(C_g^{NL}u_{gt}+\sum_{s\in\mathcal{S}_g}C_{gs}^{SU}\delta_{gst}+C_g^{SD}z_{gt}\right)$$

$$+\sum_{\omega\in\Omega}\pi_\omega\left(\sum_{t\in\mathcal{T}}\sum_{g\in\mathcal{G}}F_g(P_{gt\omega})+\sum_{t\in\mathcal{T}}\sum_{b\in\mathcal{B}}C^{LOL}L_{bt\omega}^{shed}\right) \quad (1)$$

$$s.t.\quad \delta_{gst}\le\sum_{i=T_{gs}^{SU}}^{T_{g,s+1}^{SU}-1}z_{g,t-i}\quad \forall g,t\in[T_{g,s+1}^{SU},T],s\in[1,S_g) \quad (2)$$

$$\sum_{s\in\mathcal{S}_g}\delta_{gst}=v_{gt}\qquad \forall g,t \quad (3)$$

$$\sum_{i=t-TU_g+1}^{t}v_{gi}\le u_{gt}\qquad \forall g,t\in[TU_g,T] \quad (4)$$

$$\sum_{i=t-TD_g+1}^{t}z_{gi}\le 1-u_{gt}\qquad \forall g,t\in[TD_g,T] \quad (5)$$

$$u_{gt}-u_{g,t-1}=v_{gt}-z_{gt}\qquad \forall g,t \quad (6)$$

$$\sum_{g\in\mathbf{G}(b)}P_{gt\omega}+\sum_{q\in\mathbf{W}(b)}W_{qt\omega}-\left(L_{bt}-L_{bt\omega}^{\text{shed}}\right)$$
$$=\sum_{l\in\mathbf{f}(b)}PL_{lt\omega}-\sum_{l\in\mathbf{t}(b)}PL_{lt\omega}\qquad \forall b,t,\omega \quad (7)$$

$$PL_{lt\omega}=(\theta_{at\omega}-\theta_{bt\omega})/x_{ab}\qquad \forall l,t,\omega \quad (8)$$

$$-PL_{lt}^{\max}\le PL_{lt\omega}\le PL_{lt}^{\max}\qquad \forall l,t,\omega \quad (9)$$

$$0\le L_{bt\omega}^{\text{shed}}\le L_{bt}\qquad \forall b,t,\omega \quad (10)$$

$$(P_{gt\omega}+r_{gt\omega})-P_{g,t-1,\omega}\le RU_g\qquad \forall g,t,\omega \quad (11)$$

$$-P_{gt\omega}+P_{g,t-1,\omega}\le RD_g\qquad \forall g,t,\omega \quad (12)$$

$$\sum_{g\in\mathcal{G}}r_{gt\omega}\ge R_t\qquad \forall t,\omega \quad (13)$$

$$P_{gt\omega}\ge P_g^{\min}u_{gt}\qquad \forall g,t,\omega \quad (14)$$

$$P_{gt\omega}+r_{gt\omega}\le P_g^{\max}u_{gt}-(P_g^{\max}-SU_g)v_{gt}\qquad \forall g,t,\omega \quad (15)$$

$$P_{gt\omega}+r_{gt\omega}\le P_g^{\max}u_{gt}-(P_g^{\max}-SD_g)z_{g,t+1}\qquad \forall g,t,\omega \quad (16)$$

In the above formulation, constraints (2) and (3) are startup cost constraints. They choose the suitable startup-type variable δ_{gst} that activates the corresponding startup cost C_{gs}^{SU} in the objective function of (1). Constraints (4) and (5) are the minimum uptime and downtime constraints. Constraint (6) is a logical constraint guaranteeing that v_{gi} and z_{gi} have proper values at the startup and shutdown time. Constraints (7), (8) and (9) are to meet the power balance and network transmission security requirements. Constraint (10) describes the load shedding. Constraints (11), (12) and (13) refer to the ramping limitation and spinning reserve requirement. Constraints (14), (15) and (16) denote the minimum and maximum generation limitations.

B. Proposed Data-driven Stochastic SCUC Model

It should be noted that the probability distribution of wind power is important to generate scenarios. However, the uncertainties should be considered in the system modeling. In this way, the unknown probability distribution of wind power follows any possible probability distribution within a pre-defined confidence set built up upon the historical data.

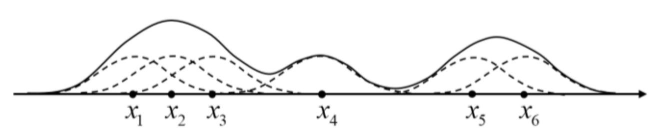

This article has been accepted for publication in a future issue of this journal, but has not been fully edited. Content may change prior to final publication. Citation information: DOI 10.1109/TSTE.2018.2825361, IEEE Transactions on Sustainable Energy

Fig. 4. Uncertain probability distribution functions.

As shown in Fig. 4, the possible probability distributions are fully covered by the confidence set. Here, we consider that the pre-defined confidence set Ψ is convex, which can facilitate the computation. In the prior-art research, two methods were reported to construct the confidence set. One is based on the first- and second-order moments (e.g., mean and variance). The other is to utilize the density information (e.g., norm-1 and norm-*inf*). In this paper, the latter is adopted for illustration and the two confidence sets can be expressed as

$$\Psi_1 = \{\pi_\omega | \|\pi_\omega - \pi_\omega^0\|_1 \le \beta\} = \left\{\pi_\omega \middle| \sum_{\omega\in\Omega} |\pi_\omega - \pi_\omega^0| \le \beta \right\} \tag{17a}$$

$$\Psi_\infty = \{\pi_\omega | \|\pi_\omega - \pi_\omega^0\|_\infty \le \beta\} = \left\{\pi_\omega \middle| \max_{\omega\in\Omega} |\pi_\omega - \pi_\omega^0| \le \beta \right\} \tag{17b}$$

It has been studied in [39] that the estimated probability distribution will approach the true probability distribution if more historical data can be obtained. For a pre-designed confidence level α and the controllable parameter for the confidence set β can be calculated as

$$\beta_{\Psi_1} = \frac{N_s}{2K} \ln \frac{2N_s}{1-\alpha}, \quad \beta_{\Psi_\infty} = \frac{1}{2K} \ln \frac{2N_s}{1-\alpha} \tag{18}$$

For each given probability distribution, the stochastic SCUC model can be solved by (1)-(16). The confidence set actually gives a series of estimated probability distributions of wind power that will give a series of stochastic SCUC solutions. In order to protect the system against all the possible stochastic SCUC solutions resulted from the uncertain probability distribution of wind power. A data-driven stochastic SCUC model aims to find the optimal solution under the worst-case probability distribution, such that

$$\min_{u_{gt}, v_{gt}, \delta_{gst}, z_{gt}} \sum_{t\in\mathcal{T}} \sum_{g\in\mathcal{G}} \left(C_g^{NL} u_{gt} + \sum_{s\in\mathcal{S}_g} C_{gs}^{SU} \delta_{gst} + C_g^{SD} z_{gt} \right) + \max_{\pi_\omega\in\Psi} \min_{P_{gt\omega}, L_{bt\omega}^{shed}} \sum_{\omega\in\Omega} \pi_\omega \sum_{t\in\mathcal{T}} \left(\sum_{g\in\mathcal{G}} F_g(P_{gt\omega}) + \sum_{b\in\mathcal{B}} C^{LOL} L_{bt\omega}^{shed} \right) \tag{19}$$

$$\text{s.t.} \quad (2)\text{-}(16) \tag{20}$$

The above proposed data-driven stochastic SCUC model can be essentially cast as a two-stage optimization problem. Here, the first-stage optimizes the unit commitment, while the second-stage optimization is to find the worst-case operational cost and the load loss under different probability distributions of wind power.

IV. Duality-Free Decomposition Method

The data-driven stochastic unit commitment model proposed in this paper can be solved by the Bender's decomposition method or the standard column-and-constraint generation method [20], [23], [45]-[46], which is implemented in a master sub-problem framework. That is, the sub-problem aims to find the critical scenario of the uncertain set that provides an upper bound. Then, new variables and constraints are added to the master problem to obtain a lower bound. The master problem and sub-problem are solved iteratively and the method stops until the gap between the upper and lower bounds is smaller than a pre-set convergence tolerance.

A. Sub-problems

For a given set of specific first-stage variables in the *k*-th iteration as $(u_{gt}^*, v_{gt}^*, \delta_{gst}^*, z_{gt}^*)$, we can establish a second-stage bi-level "max-min" model from (19)-(20) to find the worst-case scenario, yielding

$$\max_{\pi_\omega\in\Psi} \min_{\substack{P_{gt\omega}, L_{bt\omega}^{shed},\\ PL_{lt\omega}, \theta_{t\omega}, r_{gt\omega}}} \sum_{\omega\in\Omega} \pi_\omega \sum_{t\in\mathcal{T}} \left(\sum_{g\in\mathcal{G}} F_g(P_{gt\omega}) + \sum_{b\in\mathcal{B}} C^{LOL} L_{bt\omega}^{shed} \right) \tag{21}$$

$$s.t. \quad \sum_{g\in\mathbf{G}(b)} P_{gt\omega} + \sum_{q\in\mathbf{W}(b)} W_{qt\omega} - \left(L_{bt} - L_{bt\omega}^{\text{shed}}\right) = \sum_{l\in\mathbf{f}(b)} PL_{lt\omega} - \sum_{l\in\mathbf{t}(b)} PL_{lt\omega} \quad \forall b,t,\omega \tag{22}$$

$$PL_{lt\omega} = (\theta_{at\omega} - \theta_{bt\omega})/x_{ab} \quad \forall l,t,\omega \tag{23}$$

$$-PL_{lt}^{\max} \le PL_{lt\omega} \le PL_{lt}^{\max} \quad \forall l,t,\omega \tag{24}$$

$$0 \le L_{bt\omega}^{\text{shed}} \le L_{bt} \quad \forall b,t,\omega \tag{25}$$

$$\left(P_{gt\omega} + r_{gt\omega}\right) - P_{g,t-1,\omega} \le RU_g \quad \forall g,t,\omega \tag{26}$$

$$-P_{gt\omega} + P_{g,t-1,\omega} \le RD_g \quad \forall g,t,\omega \tag{27}$$

$$\sum_{g\in\mathcal{G}} r_{gt\omega} \ge R_t \quad \forall t,\omega \tag{28}$$

$$P_{gt\omega} \ge P_g^{\min} u_{gt}^{k*} \quad \forall g,t,\omega \tag{29}$$

$$P_{gt\omega} + r_{gt\omega} \le P_g^{\max} u_{gt}^* - \left(P_g^{\max} - SU_g\right) v_{gt}^* \quad \forall g,t,\omega \tag{30}$$

$$P_{gt\omega} + r_{gt\omega} \le P_g^{\max} u_{gt}^* - \left(P_g^{\max} - SD_g\right) z_{g,t+1}^* \quad \forall g,t,\omega \tag{31}$$

The sub-problem is a "max-min" bi-level problem and we can dualize the inner "min" model to obtain its equivalent "max" model based on the strong duality theory. Then, the bi-level model can be reformulated as a single "max" linear programming model. However, the dual problem is actually a large-scale optimization model, especially when the number of scenarios is large. It may significantly affect the computational performance and online applications.

Fortunately, it has been found that the second-stage bi-level "max-min" model has a special structure and thus it can be decomposed into several small sub-problems without the duality information. Since the feasible region enclosed by the second-stage variables is disjoint with the confidence set Ψ, the summation operator "Σ" and "min" operator can be exchanged. Thus, the second-stage "max-min" problem can be formulated as

$$\max_{\pi_\omega\in\Psi} \sum_{\omega\in\Omega} \pi_\omega \min_{\substack{P_{gt\omega}, L_{bt\omega}^{shed},\\ PL_{lt\omega}, \theta_{t\omega}, r_{gt\omega}}} \sum_{t\in\mathcal{T}} \left(\sum_{g\in\mathcal{G}} F_g(P_{gt\omega}) + \sum_{b\in\mathcal{B}} C^{LOL} L_{bt\omega}^{shed} \right) \tag{32}$$

$$s.t. \quad (7)\text{-}(16) \tag{33}$$

Furthermore, let $h_\omega = \min_{\substack{P_{gt\omega}, L_{bt\omega}^{shed},\\ PL_{lt\omega}, \theta_{t\omega}, r_{gt\omega}}} \sum_{t\in\mathcal{T}} \left(\sum_{g\in\mathcal{G}} F_g(P_{gt\omega}) + \sum_{b\in\mathcal{B}} C^{LOL} L_{bt\omega}^{shed} \right)$ and the model (32)-(33) becomes

$$\max_{\pi_\omega\in\Psi} \sum_{\omega\in\Omega} \pi_\omega h_\omega \tag{34}$$

$$s.t. \quad h_\omega = \min_{P_{gt\omega}, L_{bt\omega}^{shed}, PL_{lt\omega}, \theta_{t\omega}, r_{gt\omega}} \sum_{t\in\mathcal{T}} \left(\sum_{g\in\mathcal{G}} F_g(P_{gt\omega}) + \sum_{b\in\mathcal{B}} C^{LOL} L_{bt\omega}^{shed} \right) \tag{35}$$

$$s.t.\quad (7)\text{-}(16) \tag{36}$$

If there are N_s scenarios, the lower-level model of the bi-level problem can be decomposed into N_s independent optimization models. Especially, the feasible region Ψ for the upper level and the feasible region for the lower level are absolutely disjoint, resulting in a decoupled strategy.

For each scenario, it gives a linear programming model as

$$h_\omega^{k*} = \min_{\substack{P_{gt\omega}, L_{bt\omega}^{shed}, \\ PL_{lt\omega}, \theta_{t\omega}, r_{gt\omega}}} \sum_{t\in\mathcal{T}} \left(\sum_{g\in\mathcal{G}} F_g(P_{gt\omega}) + \sum_{b\in\mathcal{B}} C^{LOL} L_{bt\omega}^{shed} \right) \tag{37}$$

$$s.t.\quad (7)\text{-}(16) \tag{38}$$

When the optimal solution $\left(h_1^{k*}, \dots, h_\omega^{k*} \dots, h_{N_s}^{k*}\right)$ is obtained, it gives

$$\max_{\pi_\omega \in \Psi} \sum_{\omega\in\Omega} \pi_\omega h_\omega^{k*} \tag{39}$$

Thus, the original bi-level model can be solved by N_s+1 small linear programming models, where N_s models described in (4) can be handled in parallel. The proposed method does not need to dualize the inner model when solving the bi-level sub-problem, and thus it is referred to as a duality-free decomposition method. A simple example for the "max-min" sub-problem is shown in Appendix to verify the proposed duality-free decomposition method.

B. Master Problem

When the sub-problem is solved, an optimal value $\vartheta\left(P_{gt\omega}^{k*}, L_{bt\omega}^{shed,k*}, PL_{lt\omega}^{k*}, \theta_{t\omega}^{k*}, r_{gt\omega}^{k*}\right)$ and the worst-case probability $\left(\pi_1^{k*}, \dots, \pi_\omega^{k*} \dots, \pi_{N_s}^{k*}\right)$ are obtained. In fact, this gives an upper bound for the original model. Then, a set of extra variables $\left(P_{gt\omega}^{k+1}, L_{bt\omega}^{shed,k+1}, PL_{lt\omega}^{k+1}, \theta_{t\omega}^{k+1}, r_{gt\omega}^{k+1}\right)$ and associated constraints are generated and added into the master problem by fixing the optimal probability $\left(\pi_1^{k*}, \dots, \pi_\omega^{k*} \dots, \pi_{N_s}^{k*}\right)$ from the above model in (32)-(33).

If the sub-problem is feasible, we can create variables $\left(P_{gt\omega}^{k+1}, L_{bt\omega}^{shed,k+1}, PL_{lt\omega}^{k+1}, \theta_{t\omega}^{k+1}, r_{gt\omega}^{k+1}\right)$ and assign the following constraints to the master problem with the fixed optimal probability at the k-th iteration $\left(\pi_1^{k*}, \dots, \pi_\omega^{k*} \dots, \pi_{N_s}^{k*}\right)$, which are called "optimality cuts".

$$\eta \ge \sum_{\omega\in\Omega} \pi_\omega^{k*} \sum_{t\in\mathcal{T}} \left(\sum_{g\in\mathcal{G}} F_g\left(P_{gt\omega}^{k+1}\right) + \sum_{b\in\mathcal{B}} C^{LOL} L_{bt\omega}^{shed,k+1} \right) \tag{40}$$

$$\sum_{g\in\mathbf{G}(b)} P_{gt\omega}^{k+1} + \sum_{q\in\mathbf{W}(b)} W_{qt\omega} - \left(L_{bt} - L_{bt\omega}^{shed,k+1}\right) = \sum_{l\in\mathbf{f}(b)} PL_{lt\omega}^{k+1} - \sum_{l\in\mathbf{t}(b)} PL_{lt\omega}^{k+1} \quad \forall b,t,\omega \tag{41}$$

$$PL_{lt\omega}^{k+1} = \left(\theta_{at\omega}^{k+1} - \theta_{bt\omega}^{k+1}\right)/x_{ab} \qquad \forall l,t,\omega \tag{42}$$

$$-PL_{lt}^{\max} \le PL_{lt\omega}^{k+1} \le PL_{lt}^{\max} \qquad \forall l,t,\omega \tag{43}$$

$$0 \le L_{bt\omega}^{shed,k+1} \le L_{bt} \qquad \forall b,t,\omega \tag{44}$$

$$\left(P_{gt\omega}^{k+1} + r_{gt\omega}\right) - P_{g,t-1,\omega}^{k+1} \le RU_g \qquad \forall g,t,\omega \tag{45}$$

$$-P_{gt\omega}^{k+1} + P_{g,t-1,\omega}^{k+1} \le RD_g \qquad \forall g,t,\omega \tag{46}$$

$$\sum_{g\in\mathcal{G}} r_{gt\omega}^{k+1} \ge R_t \qquad \forall t,\omega \tag{47}$$

$$P_{gt\omega}^{k+1} \ge P_g^{\min} u_{gt} \qquad \forall g,t,\omega \tag{48}$$

$$P_{gt\omega}^{k+1} + r_{gt\omega}^{k+1} \le P_g^{\max} u_{gt} - \left(P_g^{\max} - SU_g\right) v_{gt} \quad \forall g,t,\omega \tag{49}$$

$$P_{gt\omega}^{k+1} + r_{gt\omega}^{k+1} \le P_g^{\max} u_{gt} - \left(P_g^{\max} - SD_g\right) z_{g,t+1} \quad \forall g,t,\omega \tag{50}$$

where η is a dummy continuous variable.

If the sub-problem is infeasible, it is possible to create variables $\left(P_{gt\omega}^{k+1}, L_{bt\omega}^{shed,k+1}, PL_{lt\omega}^{k+1}, \theta_{t\omega}^{k+1}, r_{gt\omega}^{k+1}\right)$ and assign the following constraints to the master problem with the fixed optimal probability at the k-th iteration $\left(\pi_1^{k*}, \dots, \pi_\omega^{k*} \dots, \pi_{N_s}^{k*}\right)$, which is called "feasibility cuts".

$$\sum_{g\in\mathbf{G}(b)} P_{gt\omega}^{k+1} + \sum_{q\in\mathbf{W}(b)} W_{qt\omega} - \left(L_{bt} - L_{bt\omega}^{shed,k+1}\right) = \sum_{l\in\mathbf{f}(b)} PL_{lt\omega}^{k+1} - \sum_{l\in\mathbf{t}(b)} PL_{lt\omega}^{k+1} \quad \forall b,t,\omega \tag{51}$$

$$(42)\text{-}(50) \tag{52}$$

The master problem aims to relax the original optimization model and provide a lower bound. Mathematically, it is a standard mixed integer liner program (MILP) model that can be easily dealt with by the standard commercial solvers.

Finally, for a given gap ε, the complete procedure of the duality-free decomposition method for the data-driven stochastic unit commitment problem can be described as

Step 1: Let $LB = -\infty$, $UB = +\infty$, $K = 0$;

Step 2: Solve the master problem model:

$$\min \sum_{t\in\mathcal{T}} \sum_{g\in\mathcal{G}} \left(C_g^{NL} u_{gt} + \sum_{s\in\mathcal{S}_g} C_{gs}^{SU} \delta_{gst} + C_g^{SD} z_{gt} \right) + \eta \tag{53}$$

$$s.t.\quad (3)\text{-}(7) \tag{54}$$

$$(40)\text{-}(50) \qquad k=1,\dots,K \tag{55}$$

Solve the above model and derive the optimal solution ($u_{gt}^*, v_{gt}^*, \delta_{gst}^*, z_{gt}^*, \eta^*$; $P_{gt\omega}^{1*}, L_{bt\omega}^{shed,1*}, PL_{lt\omega}^{1*}, \theta_{t\omega}^{1*}, r_{gt\omega}^{1*}$; ... ; $P_{gt\omega}^{K*}, L_{bt\omega}^{shed,K*}, PL_{lt\omega}^{K*}, \theta_{t\omega}^{K*}, r_{gt\omega}^{K*}$) as well as the optimal objective value O^{K*}. Then, update the lower bound as $LB=O^{K*}$;

Step 3: Fix ($u_{gt}^*, v_{gt}^*, \delta_{gst}^*, z_{gt}^*$) and solve the sub-problem model in parallel by (37)-(39), respectively. If the sub-problem is feasible, let the optimal objective value be ϑ^*; otherwise set $\vartheta^* = +\infty$. Furthermore, update the upper bound as UB = min{UB, $\sum_{t\in\mathcal{T}} \sum_{g\in\mathcal{G}} \left(C_g^{NL} u_{gt}^* + \sum_{s\in\mathcal{S}_g} C_{gs}^{SU} \delta_{gst}^* + C_g^{SD} z_{gt}^* \right) + \vartheta^*$};

Step 4: If (UB–LB)≤ε, return ($u_{gt}^*, v_{gt}^*, \delta_{gst}^*, z_{gt}^*$) and stop. Otherwise, add the cuts as

(a) If the sub-problem in Step 3 is feasible, obtain the optimal probability $\left(\pi_1^{k*}, \dots, \pi_\omega^{k*} \dots, \pi_{N_s}^{k*}\right)$. Create variables $\left(P_{gt\omega}^{k+1}, L_{bt\omega}^{shed,k+1}, PL_{lt\omega}^{k+1}, \theta_{t\omega}^{k+1}, r_{gt\omega}^{k+1}\right)$ and assign the constraints (40)-(50) to the master problem;

(b) If the sub-problem in Step 3 is infeasible, create variables $\left(P_{gt\omega}^{k+1}, L_{bt\omega}^{shed,k+1}, PL_{lt\omega}^{k+1}, \theta_{t\omega}^{k+1}, r_{gt\omega}^{k+1}\right)$ and add the constraints (51)-(52) to the master problem;

Step 5: Update K=K+1 and go back to Step 2.

This article has been accepted for publication in a future issue of this journal, but has not been fully edited. Content may change prior to final publication. Citation information: DOI 10.1109/TSTE.2018.2825361, IEEE Transactions on Sustainable Energy

V. Numerical Analysis

In this section, three unit commitment models with wind power generation uncertainties are designed and compared with the proposed data-driven stochastic SCUC model (DSSCUC):

- **WSSCUC**: It is a worst-case stochastic SCUC model. Solve the general stochastic SCUC model (1)-(16) and fix the first-stage decision variables. Then, we randomly generate 1000 different probabilities from the confidence set and solve the second-stage problem for each given probability. Then, choose the solution with the maximum objective value is served as the worst-case scenario for the stochastic approaches.
- **RSCUC**: It is a two-stage robust SCUC model. Using the historical data, we can give the uncertainty set of robust optimization with respect to central limit theorem.
- **SSCUC**: It is a two-stage stochastic SCUC model.

The computation is carried on a computer with an Intel® Core™ i7 Duo Processor (2.4 GHz) and 4-GB RAM in MATLAB by the CPLEX 12.6 commercial solver. It should be noted that the series of sub-problems in the proposed method have independent mathematical structures, enabling the parallel computation. Due to the lack of hard-ware platform of high-performance computing, we use the “for” loop to simulate the parallel computation and take the worst computing time of the sub-problems as the parallel computational time.

A. Test on the IEEE 118-bus System

At first, the proposed duality-free decomposition based DSSCUC is studied on the IEEE 118-bus test system including 54 generators and 186 transmission lines [47]. The spinning reserve requirement is equal to 5% of the load demand. The cost of load shedding is $3500/MWh. Five 300-MW wind farms are located at bus #10, #25, #26, #37, and #38. Here, the historical wind data from the real-life wind farms in Northwestern China is used, as shown in Figs. 1-3.

The comparison of the three methods is presented in Table I with $N_s = 5$. It is obvious that the RSCUC model optimizes the solution that is immune against all the possible realizations, which leads to the highest optimal total cost. The SSCUC method considers the probability of scenarios, which therefore yields the lowest optimal total cost. In contrast, the proposed DSSCUC model using either β_{Ψ_1} or β_{Ψ_∞} is greater than the SSCUC, while smaller than the WSSCUC approach. When β is large enough, the solution will tend to that of the RSUCU model. On the contrary, when β is small, the solution will approach that of the SSUCU model. The DSSCUC model is between RSCUC and SSCUC. As a result, β can be considered as a budget parameter that can control the size of uncertainty sets and further a trade-off between the robust and stochastic optimization can be made. With the increase of β, the uncertainty set becomes larger and the optimal solution is more conservative.

Moreover, the worst-case total cost from the stochastic approach is computed by the WSSCUC model considering uncertain probability distribution of about 9.5%~17.2% larger than the traditional two-stage SCUC model. It is obvious that a larger confidence level α will enlarge the confidence set (i.e., β becomes large), and the worst-case solution will thus become larger. The results suggest that the traditional SSCUC model suffers from the uncertain probability distribution of wind power. However, the proposed DSSCUC model takes into account the uncertainty from the statistics, so the solution will be benefited.

Finally, the stochastic SCUC models including the SSCUC, WSSCUC and DSSCUC models are always better than the robust SCUC model. This is because the robust optimization neglects the probability of scenarios and the probability of the worst-case scenario may be very small in practice. Thus, the extreme worst case will sacrifice much cost (about 24%) to protect the system from the worst case with small probabilities. In the framework of the two-stage stochastic optimization, the expected total cost is optimized which gives the optimal solution under the given probability distribution.

Table I. Performance of Different SCUC Models.

α	Total cost/10^6\$				
	DSSCUC		RSCUC	SSCUC	WSSCUC
	ψ_1	$\psi_{\inf}$			
0.5	1.5167	1.5035	1.8453	1.4871	1.6288
0.6	1.5331	1.5201			1.6391
0.7	1.5502	1.5496			1.6536
0.8	1.5795	1.5732			1.6712
0.9	1.6111	1.5943			1.6934
0.95	1.6348	1.6132			1.7158
0.99	1.6584	1.6380			1.7433

In order to investigate the influence of the load demand and wind power output on the solution decision, we consider four seasons to study where a typical day is selected in each season. In spring, the wind power is high and the load demand is low. In summer, the wind power is low and the load demand is high. In autumn, both the wind power and load demand are low. In winter, both the wind power and load demand are high. The solutions are presented in Table II. Observations show that the total cost in spring is the lowest and the solution in summer is the highest. More importantly, the gap between DSSCUC and other methods is small when the wind power output is low, whereas it is large in the case of a high penetration of wind power.

Furthermore, the proposed duality-free decomposition method (PM) and the traditional Benders decomposition method (TM) in [39] were explicitly compared considering scenarios and the results can be found in Table III. It can be observed that for the same N_s, the PM and TM generate the same objective value (obj.). In contrast, the PM preforms an order of magnitude faster than the TM. This is because the PM needs 2-4 iterations for convergence, whereas the TM needs 9-15 iterations. Moreover, the PM yields a decomposition structure for the second-stage problem that can be handled in parallel, which can significantly reduce the computational time, especially for the problem with a large number of scenarios.

Table II. Impact of Seasons on Different SCUC Models.

Seasons	Total cost/10^6\$				
	DSSCUC		RSCUC	SSCUC	WSSCUC
	ψ_1	$\psi_{\inf}$			
Spring	1.6348	1.6132	1.8453	1.4871	1.7158
Summer	2.4045	2.3895	2.5101	2.3347	2.4690
Autumn	2.0832	2.0787	2.1576	2.0333	2.1112

Winter	1.8355	1.7911	2.3982	1.5798	2.1351

Table III. Comparison of the traditional and proposed methods.

N_s	*D*-1				*D*-inf			
	Obj. (10^6\$)		Time (min)		Obj. (10^6\$)		Time (min)	
	TM	PM	TM	PM	TM	PM	TM	PM
5	1.63	1.63	36	4	1.61	1.61	34	5
10	1.58	1.58	44	4	1.55	1.55	43	5
15	1.56	1.56	53	4	1.51	1.51	57	6
20	1.55	1.55	75	5	1.50	1.50	81	9
25	1.54	1.54	90	6	1.49	1.49	103	11

Moreover, the comparison of computational performance among the three approaches is shown in Table IV. The SSCUC is a standard MILP that can be directly handled by CPLEX. However, the computational time increases significantly with a large number of scenarios. This is because the SSCUC model contains N_s sets of decision variables and constraints. The RSUCU approach needs 7 iterations while the challenge is in the inner bi-level "max-min" problem, where a large-scale MILP is performed by the use of duality. In addition, the computational time of the SSUCU will increase significantly when the number of scenarios is increased. Among the three methods, the proposed DSSCUC model consumes the least computational time due to the duality-free decomposition method, where the second-stage "max-min" problem is decomposed into several small-scale linear programs that are handled in parallel. It should be noted that the increase of N_s will increase its computational time. The reason is that the master problem will become larger with a large number of scenarios.

Table IV. Comparison of computational efficiency by three methods on 118-bus test system (min).

N_s	DSSCUC		RSCUC	SSCUC
	D-inf	*D*-1		
5	4	5		12
10	4	5		19
15	4	6	10	29
20	5	9		47
25	6	11		78

B. Test on the Practical Hainan Power Grid in China

To verify the proposed method on a large-scale test system, the Hainan power grid in China is used, which is depicted in Fig. 5. This power grid contains 82 generators with the total capacity being 5300 MW, 7 wind farms with the total capacity being 800 MW, and the load demand is 4200 MW. The transmission network is operated on two voltage levels, i.e., 220 kV and 500 kV, where there are 34 high-voltage substations and 404 transmission corridors.

The per unit values of the forecasted load demand and wind power generation over 24 hours are shown in Fig. 6, which are defined by P^t/P^0. Here, P^t is the value at the time period t and P^0 is the value at 1:00 AM. We consider the true wind power follows a multivariate normal distribution with the variance equivalent to 1/3 of the forecasted value. Furthermore, 1000 samples are generated as the set of the historical data. The sensitivity analysis of parameters on the four models is presented in Table V. For each group, we consider four points for comparison. The results reveal that with the increase of the number of scenarios N_s and confidence level α and with the decrease of the number of historical data K, the total cost will become larger since the uncertainty set becomes larger. Thus, it is suggested that for a given confidence level and the number of scenarios, more historical data can narrow the region of the uncertainty set and reduce the conservativeness. Similarly, for a given number of scenarios and historical data, improving the confidence level indicates that the system requires higher estimation precision for the possible probability distributions. In that case, the confidence set and the uncertainty set become larger. Moreover, it can be observed in Fig. 7 that the gap between WSSCUC and DSSCUC will become smaller if α and K are increased while decreasing N_s.

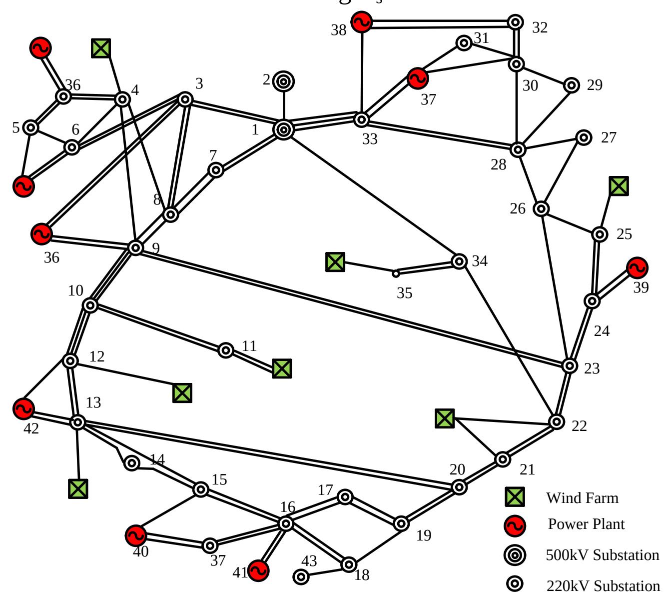

Fig. 5. Layout of the Hainan power grid in China.

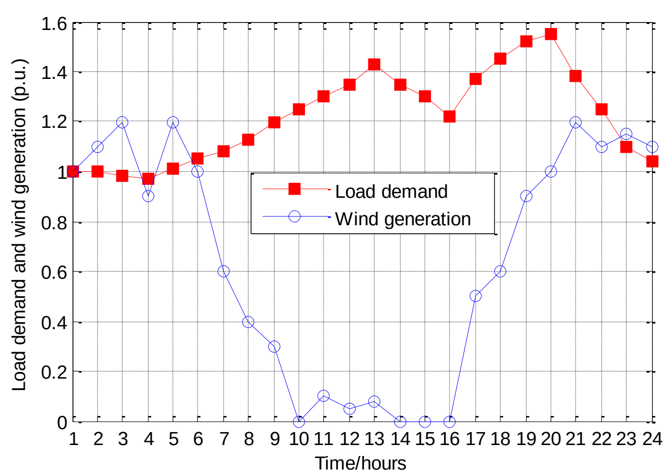

Fig. 6. Load demand and wind generation over 24 hours

Finally, the computational performance among the three approaches on the Hainan power grid is shown in Table VI. The comparison demonstrates that the simulation results in Table IV are similar to those in Table VI. The computational time increases significantly with a large number of scenarios. As for the MILP problem, the computational time mainly depends on

This article has been accepted for publication in a future issue of this journal, but has not been fully edited. Content may change prior to final publication. Citation information: DOI 10.1109/TSTE.2018.2825361, IEEE Transactions on Sustainable Energy

the number of variables and constraints. If N_s = 25, the traditional method cannot find the optimal solution within 1000 minutes. If N_s = 50, the number of variables is more than one million and the number of constraints are more than five millions. Hence, the traditional method for the DSSCUC cannot be solved due to the limited memory space. In contrast, the proposed duality-free decomposition based method can still handle the DSSCUC and the computational speed is improved up to two orders of magnitudes, since the large-scale problem is decomposed into several small-scale sub-problems.

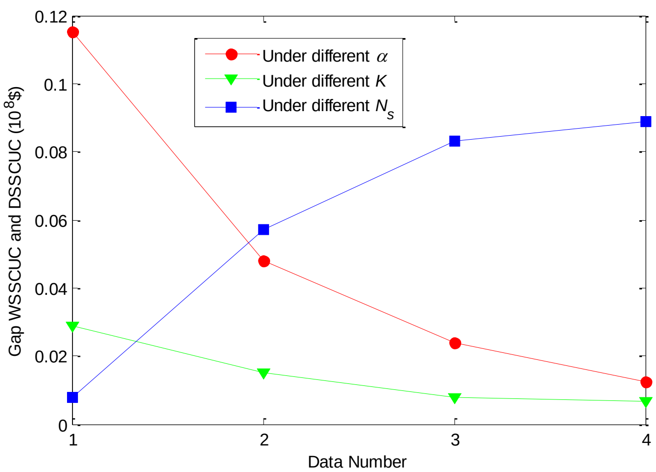

Fig. 7. Gap between WSSCUC and DSSCUC.

Table V. Sensitivity analysis of parameters

α (K=1000 N_s=10)	Total cost/10^8\$				
	DSSCUC		RSCUC	SSCUC	WSSCUC
	ψ_1	$\psi_{\inf}$			
0.5	3.5629	3.5432	4.5158	3.2494	3.6783
0.90	3.6649	3.6513			3.7130
0.95	3.7031	3.6943			3.7271
0.99	3.7806	3.7745			3.7932
K (α =0.95 N_s=10)	Total cost/10^8\$				
	DSSCUC		RSCUC	SSCUC	WSSCUC
	ψ_1	$\psi_{\inf}$			
1000	3.7031	3.6619	4.5158	3.2494	3.7321
3000	3.4313	3.4106			3.4465
6000	3.3586	3.3417			3.3663
10000	3.2989	3.2833			3.3056
N_s (α =0.95 K=1000)	Total cost/10^8\$				
	DSSCUC		RSCUC	SSCUC	WSSCUC
	ψ_1	$\psi_{\inf}$			
5	3.4854	3.341	4.5158	3.2494	3.4933
10	3.7031	3.562			3.7603
25	4.0515	3.918			4.1345
50	4.3054	4.195			4.3942

Table VI. Comparison of computational efficiency by three methods on Hainan power grid in China (min).

N_s	DSCUC		RSCUC	SSCUC
	TM	PM		
5	92	12	78	34
10	342	12		78
25	>1000	13		375
50	out of memory	13		>1000
100	out of memory	15		out of memory

Conclusions

To address the uncertain probability distribution of wind power resultant from the historical data, a data-driven stochastic security-constrained unit commitment was set up to optimize the unit commitment under the worst probability distribution in this paper. Furthermore, a novel duality-free decomposition method was proposed for the data-driven stochastic security-constrained unit commitment. The key point is that the second-stage sub-problem has a special structure that can be decomposed into several parallel sub-problems without the duality information. However, it is required by the traditional Bender's decomposition method. Numerical results have shown that the proposed method performs better than the Benders decomposition method especially for the problem with a large number of scenarios.

Appendix

A Simple Example for the Sub-problem

In order to verify the proposed duality-free decomposition method, we set up a simple example with two variables (x_1, x_2) under three scenarios to show the detail numerical results. The bi-level sub-problem is formulated as

$$\max_{p_1,p_2,p_3}\min_{x_1,x_2}\ \left(2x_1^1+3x_2^1\right)p_1+\left(2x_1^2+3x_2^2\right)p_2+\left(2x_1^3+3x_2^3\right)p_3 \quad \text{(A1)}$$

$$\begin{aligned} s.t.\quad & x_1^1+x_2^1=1,\quad x_1^2+x_2^2=2,\quad x_1^3+x_2^3=3 \\ & x_1^1,x_2^1,x_1^2,x_2^2,x_1^3,x_2^3\ge 0 \end{aligned} \quad \text{(A2)}$$

$$\begin{aligned} & p_1\in[0.1,0.3],\ p_2\in[0.4,0.7],\ p_3\in[0.2,0.6], \\ & p_1+p_2+p_3=1 \end{aligned} \quad \text{(A3)}$$

Traditional method dualizes the inner "min" model to obtain its equivalent "max" model based on the strong duality theory. Then, the bi-level model can be reformulated as a single "max" linear programming model, such that

$$\max_{p_1,p_2,p_3,\lambda_1,\lambda_2,\lambda_3}\quad \lambda_1+2\lambda_2+3\lambda_3 \quad \text{(A4)}$$

$$s.t.\quad \lambda_1\le 2p_1,\ \lambda_1\le 3p_1,\ \lambda_2\le 2p_2,\ \lambda_2\le 3p_2,\ \lambda_3\le 2p_3,\ \lambda_3\le 3p_3 \quad \text{(A5)}$$

$$\begin{aligned} & p_1\in[0.1,0.3],\ p_2\in[0.4,0.7],\ p_3\in[0.2,0.6], \\ & p_1+p_2+p_3=1 \end{aligned} \quad \text{(A6)}$$

where λ_1, λ_2 and λ_3 are multipliers to the constraints (A2). It can be found that the above optimization model is a simple linear problem that can be solved to the global optimal solution with (p_1=0.1, p_2=0.4, p_3=0.5, λ_1=0.2, λ_2=0.8, λ_3=1.0) and the optimal objective value is 4.8.

For the proposed duality-free decomposition method, we can solve three small models by (37)-(38) in parallel, such that

$$\min_{x_1^1,x_2^1}\quad 2x_1^1+3x_2^1 \quad \text{(A7-a)}$$

$$s.t.\quad x_1^1+x_2^1=1,\ x_1^1,x_2^1\ge 0 \quad \text{(A7-b)}$$

The global optimal solution is $\left(x_1^1=1,x_2^1=0\right)$ and the optimal objective value is h_1=2.

$$\min_{x_1^2,x_2^2}\quad 2x_1^2+3x_2^2 \quad \text{(A8-a)}$$

$$s.t.\quad x_1^2+x_2^2=2,\ x_1^2,x_2^2\ge 0 \quad \text{(A8-b)}$$

The global optimal solution is $\left(x_1^2 = 2, x_2^2 = 0\right)$ and the optimal objective value is h_2=4.

$$\min_{x_1^3, x_2^3} \quad 2x_1^3 + 3x_2^3 \tag{A9-a}$$

$$s.t. \quad x_1^3 + x_2^3 = 3,\ x_1^3, x_2^3 \ge 0 \tag{A9-b}$$

The global optimal solution is $\left(x_1^3 = 3, x_2^3 = 0\right)$ and the optimal objective value is h_3=6.

Furthermore, we solve another small linear program by (39), using the information from (A7)-(A9), such that

$$\max_{p_1, p_2, p_3} \quad h_1 p_1 + h_2 p_2 + h_3 p_3 \tag{A10-a}$$

$$\begin{aligned} s.t. \quad & p_1 \in [0.1, 0.3],\ p_2 \in [0.4, 0.7],\ p_3 \in [0.2, 0.6], \\ & p_1 + p_2 + p_3 = 1 \end{aligned} \tag{A10-b}$$

The optimal solution of the above model is (p_1=0.1, p_2=0.4, p_3=0.5) and the optimal objective value is 4.8, which is the same as the traditional method.

It can be concluded that the optimal solution and optimal objective value by the proposed method is absolutely the same as those by the traditional method, which verifies the effectiveness of the proposed method. Moreover, it can be observed that the models (A7), (A8) and (A9) are independent that can be solved in parallel. Besides, the proposed model only needs to solve 4 small linear programs comparing to the traditional method that needs to solve one large-scale optimization model.

REFERENCES

[1] J. Wang, M. Shahidehpour and Z. Li, "Security-Constrained Unit Commitment With Volatile Wind Power Generation," *IEEE Trans. Power Syst.*, vol. 23, no. 3, pp. 800-811, 2008.

[2] Y. Fu, Z. Li, and L. Wu, "Modeling and solution of the large-scale security-constrained unit commitment," *IEEE Transactions on Power Systems*, vol. 28, no. 4, pp. 3524-3533, 2013.

[3] Y. Fu, M. Shahidehpour, "Fast SCUC for Large-Scale Power Systems," *IEEE Transactions on Power Systems*, vol. 22, no. 4, pp. 2144-2151, 2007.

[4] C. Lowery and M. O'Malley, "Impact of Wind Forecast Error Statistics Upon Unit Commitment," *IEEE Trans. Sust. Energy*, vol. 3, no. 4, pp. 760-768, 2012.

[5] Y. Wang, Q. Xia, and C. Kang, "Unit Commitment With Volatile Node Injections by Using Interval Optimization," *IEEE Trans. Power Syst* , vol. 26, no. 3, pp. 1705-1713, 2011.

[6] Y. Dvorkin, H. Pandzic, M. A. Ortega-Vazquez, and D. S. Kirschen, "A Hybrid Stochastic/Interval Approach to Transmission-Constrained Unit Commitment," *IEEE Trans. Power Syst.*, vol. 30, no. 2, pp. 621-631, 2015.

[7] L. Wu, M. Shahidehpour, and T. Li, "Stochastic Security-Constrained Unit Commitment," *IEEE Trans. Power Syst.*, vol. 22, no. 2, pp. 800-811, 2007.

[8] J. M. Morales, A. J. Conejo, and J. Perez-Ruiz, "Economic Valuation of Reserves in Power Systems With High Penetration of Wind Power," *IEEE Trans. Power Syst.*, vol. 24, no. 2, pp. 900-910, 2009.

[9] F. Bouffard and F. D. Galiana, "Stochastic Security for Operations Planning With Significant Wind Power Generation," *IEEE Trans. Power Syst.*, vol. 23, no. 2, pp. 306-316, 2008.

[10] Q. P. Zheng, J. Wang, and A. L. Liu, "Stochastic Optimization for Unit Commitment - A Review," *IEEE Trans. Power Syst.*, vol. 30, no. 4, pp. 1913-1924, 2015.

[11] A. Tuohy, P. Meibom, E. Denny, and M. O'Malley, "Unit Commitment for Systems With Significant Wind Penetration," *IEEE Trans. Power Syst.*, vol. 24, no. 2, pp. 592-601, 2009.

[12] C. De Jonghe, B. F. Hobbs, and R. Belmans, "Value of Price Responsive Load for Wind Integration in Unit Commitment," *IEEE Trans. Power Syst.* , vol. 29, no. 2, pp. 675-685, 2014.

[13] J. Wang, A. Botterud, R. Bessa, H. Keko *et al.*, "Wind Power Forecasting Uncertainty and Unit Commitment," *Appl. Energy*, vol. 88, no. 11, pp. 4014-4023, 2011.

[14] A. Papavasiliou, S. S. Oren, and R. P. O'Neill, "Reserve Requirements for Wind Power Integration: A Scenario-Based Stochastic Programming Framework," *IEEE Trans. Power Syst.*, vol. 26, no. 4, pp. 2197-2206, 2011.

[15] D. Bertsimas, E. Litvinov, X. A. Sun, J. Zhao *et al.*, "Adaptive Robust Optimization for the Security Constrained Unit Commitment Problem," *IEEE Trans. Power Syst.*, vol. 28, no. 1, pp. 52-63, 2013.

[16] C. Zhao, J. Wang, J. P. Watson, and Y. Guan, "Multi-Stage Robust Unit Commitment Considering Wind and Demand Response Uncertainties," *IEEE Trans. Power Syst.*, vol. 28, no. 3, pp. 2708-2717, 2013.

[17] R. Jiang; J. Wang; Y. Guan, "Robust Unit Commitment With Wind Power and Pumped Storage Hydro," *IEEE Trans. Power Syst.*, vol. 27, no. 2, pp. 800 - 810, 2012.

[18] N. Amjady, S. Dehghan, A. Attarha and A. J. Conejo, "Adaptive Robust Network-Constrained AC Unit Commitment," *IEEE Trans. Power Syst* , vol. 32, no. 1, pp. 672 - 683, 2017.

[19] A. Kalantari, J. F. Restrepo, and F. D. Galiana, "Security-Constrained Unit Commitment With Uncertain Wind Generation: The Loadability Set Approach," *IEEE Trans. Power Syst.*, vol. 28, no. 2, pp. 1787-1796, 2013.

[20] B. Zeng and L. Zhao, "Solving two-stage robust optimization problems using a column-and-constraint generation method," *Operations Research Letters*, vol. 41, no. 5, pp. 457-461, 2013.

[21] H. Ye and Z. Li, "Robust Security-Constrained Unit Commitment and Dispatch With Recourse Cost Requirement," *IEEE Trans. Power Syst.*, vol. 31 no. 5, pp. 3527 - 3536, 2016.

[22] Y. Guan and J. Wang, "Uncertainty Sets for Robust Unit Commitment," *IEEE Trans. Power Syst.*, vol. 29, no. 3, pp. 1439-1440, 2014.

[23] Y. An and B. Zeng, "Exploring the Modeling Capacity of Two-Stage Robust Optimization: Variants of Robust Unit Commitment Model," *IEEE Trans. Power Syst.*, vol. 30, no. 1, pp. 109-122, 2015.

[24] Á. Lorca and X. Sun, "Multistage Robust Unit Commitment With Dynamic Uncertainty Sets and Energy Storage," *IEEE Trans. Power Syst.*, vol. 32, no. 3, pp. 1678 - 1688, 2017.

[25] R. Jiang, J. Wang, M. Zhang and Y. Guan, "Two-Stage Minimax Regret Robust Unit Commitment," *IEEE Trans. Power Syst.*, vol. 28, no. 3, pp. 2271 - 2282, 2013.

[26] C. Wang, F. Liu, J. Wang and et al, "Robust Risk-Constrained Unit Commitment With Large-Scale Wind Generation: An Adjustable Uncertainty Set Approach," *IEEE Trans. Power Syst.*, vol. 32, no. 1, pp. 723 - 733, 2017.

[27] C. Zhao and Y. Guan, "Unified Stochastic and Robust Unit Commitment," *IEEE Trans. Power Syst.*, vol. 28, no. 3, pp. 3353 - 3361, 2013.

[28] Q. Wang, Y. Guan, and J. Wang, "A Chance-Constrained Two-Stage Stochastic Program for Unit Commitment With Uncertain Wind Power Output," *IEEE Trans. Power Syst.*, vol. 27, no. 1, pp. 206-215, 2012.

[29] D. Pozo and J. Contreras, "A Chance-Constrained Unit Commitment With an N-k Security Criterion and Significant Wind Generation," *IEEE Trans. Power Syst.*, vol. 28, no. 3, pp. 2842-2851, 2013.

[30] H. Wu, M. Shahidehpour, Z. Li, and W. Tian, "Chance-Constrained Day-Ahead Scheduling in Stochastic Power System Operation," *IEEE Trans. Power Syst.*, vol. 29, no. 4, pp. 1583-1591, 2014.

[31] Y. Huang, Q. P. Zheng, and J. Wang, "Two-stage stochastic unit commitment model including non-generation resources with conditional value-at-risk constraints," *Electr. Power Syst. Res.*, vol. 116, no. 1, pp. 427-438, 2014.

[32] A. J. Conejo, F. J. Nogales, J. M. Arroyo, and R. Garcia-Bertrand, "Risk-constrained self-scheduling of a thermal power producer," *IEEE Trans. Power Syst.*, vol. 19, no. 3, pp. 1569-1574, 2004.

[33] Q. Wang, J. Wang, and Y. Guan, "Stochastic Unit Commitment With Uncertain Demand Response," *IEEE Trans. Power Syst.*, vol. 28, no. 1, pp. 562-563, 2013.

[34] R. A. Jabr, "Robust self-scheduling under price uncertainty using conditional value-at-risk," *IEEE Trans. Power Syst.*, vol. 20, no. 4, pp. 1852-1858, 2005.

[35] Z. Wang, Q. Bian, H. Xin and D. Gan, "A distributionally robust co-ordinated reserve scheduling model considering CVaR-based wind power reserve requirements," *IEEE Trans. Sustain. Energy*, vol. 7, no. 2, pp. 625-636, 2016.

[36] Y. Zhang, S. Shen and J. L. Mathieu, "Distributionally robust chance-constrained optimal power flow with uncertain renewables and uncertain reserves provided by loads," *IEEE Trans. Power Syst.*, vol. PP, no. 99, pp. 1-1, 2016.

[37] W. Wei, F. Liu and S. Mei, “Distributionally robust co-optimization of energy and reserve dispatch,” *IEEE Trans. Sustain. Energy*, vol. 7, no. 1, pp. 289-300, 2016.
[38] Q. Bian, H. Xin, Z. Wang, D. Gan and K. P. Wong, “Distributionally robust solution to the reserve scheduling problem with partial information of wind power,” *IEEE Trans. Power Syst.*, vol. 30, no. 5, pp. 2822-2823, 2015.
[39] C. Zhao and Y. Guan, “Data-driven stochastic unit commitment for integrating wind generation”, *IEEE Trans. Power Syst*., vol. 31, no. 4, pp. 2587-2596, 2016.
[40] P. Xiong, P. Jirutitijaroen and C. Singh, “A distributionally robust optimization model for unit commitment considering uncertain wind power generation,” *IEEE Trans. Power Syst.*, vol. 32, no. 7, pp. 39 - 49, 2017.
[41] M. Khanabadi, Y. Fu, and L. Gong, "A Fully Parallel Stochastic Multiarea Power System Operation Considering Large-Scale Wind Power Integration," *IEEE Transactions on Sustainable Energy*, vol. 9, no. 1, pp. 138-147, 2018.
[42] M. Doostizadeh, F. Aminifar, H. Lesani, and H. Ghasemi, "Multi-area market clearing in wind-integrated interconnected power systems: A fast parallel decentralized method," *Energy Conversion and Management*, vol. 113, pp. 131-142, 2016.
[43] P. Pinson, H. Madsen, H. A. Nielsen, G. Papaefthymiou et al., “From probabilistic forecasts to statistical scenarios of short-term wind power production,” *Wind Energy*, vol. 12, no. 1, pp. 51-62, 2009.
[44] J. Dupačová, N. Gröwe-Kuska, and W. Römisch, “Scenario reduction in stochastic programming,” *Mathematical Programming*, vol. 95, no. 3, pp. 493-511, 2003.
[45] B. Hu and L. Wu, "Robust SCUC Considering Continuous/Discrete Uncertainties and Quick-Start Units: A Two-Stage Robust Optimization With Mixed-Integer Recourse," *IEEE Transactions on Power Systems*, vol. 31, no. 2, pp. 1407 - 1419, 2016.
[46] T. Ding, S. Liu, W. Yuan and et al, " A Two-Stage Robust Reactive Power Optimization Considering Uncertain Wind Power Integration in Active Distribution Networks," *IEEE Transactions on Sustainable Energy*, vol. 7, no. 1, pp. 301 - 311, 2016.
[47] R. D. Zimmerman, C. E. Murillo-Sánchez, and R. J. Thomas, "MATPOWER: Steady-State Operations, Planning, and Analysis Tools for Power Systems Research and Education," *IEEE Trans. Power Syst.*, vol. 26, no. 1, pp. 12-19, Feb 2011.

Tao Ding (S’13–M’15) received the B.S.E.E. and M.S.E.E. degrees from Southeast University, Nanjing, China, in 2009 and 2012, respectively, and the Ph.D. degree from Tsinghua University, Beijing, China, in 2015. During 2013 and 2014, he was a Visiting Scholar in the Department of Electrical Engineering and Computer Science, University of Tennessee, Knoxville, TN, USA. He is currently an Associate Professor in the State Key Laboratory of Electrical Insulation and Power Equipment, the School of Electrical Engineering, Xi’an Jiaotong University. His current research interests include electricity markets, power system economics and optimization methods, and power system planning and reliability evaluation. He has published more than 60 technical papers and authored by “Springer Theses” recognizing outstanding Ph.D. research around the world and across the physical sciences—*Power System Operation with Large Scale Stochastic Wind Power Integration*. He received the excellent master and doctoral dissertation from Southeast University and Tsinghua University, respectively, and Outstanding Graduate Award of Beijing City. Dr. Ding is an Associate Editor of CSEE Journal of Power and Energy Systems.

Qingrun Yang (S’17) received the B.S. degree from the School of Electrical Engineering, Xi’an Jiaotong University, Xi’an, China, in 2016. He is currently working toward the M.S. degree at Xi’an Jiaotong University. His major research interests include power system optimization and renewable energy integration.

Xiyuan Liu (S’15) received the B.S. degree from the School of Electrical Engineering, Xi’an Jiaotong University, Xi’an, China, in 2012. She is currently working toward the Ph.D. degree at Xi’an Jiaotong University. Her major research interests include electric vehicle and optimization.

Can Huang (GS’13–M’16) received the B.S.E.E degree from Hohai university, Nanjing, China, in 2008, the M.S.E.E. degree from Southeast University, Nanjing, in 2011, and the Ph.D. degree from The University of Tennessee, Knoxville, TN, USA, in 2016. From 2011 to 2012, he was with the State Grid Electric Power Research Institute (NARI Group Corporation), Nanjing. He is currently a Postdoctoral Research Staff Member with the Lawrence Livermore National Laboratory, Livermore, CA, USA. His current research interests include advanced control, computing, and communication for power and energy systems.

Yongheng Yang (S'11-M'15-SM'17) received the B.Eng. degree in electrical engineering and automation from Northwestern Polytechnical University, Shaanxi, China, in 2009 and the Ph.D. degree in electrical engineering from Aalborg University, Aalborg, Denmark, in 2014. He was a postgraduate student at Southeast University, China, from 2009 to 2011. In 2013, he was a Visiting Scholar at Texas A&M University, USA. Dr. Yang has been with the Department of Energy Technology, Aalborg University since 2014, first as a Postdoc researcher, then an Assistant Professor, and now an Associate Professor. He has been focusing on grid integration of renewable energies, power electronic converter design, analysis and control, and reliability in power electronics. Dr. Yang served as a Guest Associate Editor of IEEE Journal of Emerging and Selected Topics in Power Electronics and a Guest Editor of Applied Sciences. He is an Associate Editor of CPSS Transactions on Power Electronics and Applications.

Min Wang received the B.S.E.E. and M.S.E.E. degrees from the Department of Electrical Engineering, Tsinghua University, Beijing, China, in 2009 and 2012, respectively. She is currently working at the Shaanxi Electric Power Corporation Economic Research Institute. Her major research interests include distribution network analysis and renewable energy integration.

Frede Blaabjerg (S’86–M’88–SM’97–F’03) was working toward the Ph.D. degree at Aalborg University, Aalborg, Denmark from 1988 to 1992. He was with ABB-Scandia, Randers, Denmark, from 1987 to 1988. He became an Assistant Professor in 1992, an Associate Professor in 1996, and a Full Professor of power electronics and drives in 1998 at Aalborg University. His current research interests include power electronics and its applications such as in wind turbines, PV systems, reliability, harmonics, and adjustable speed drives. Prof. Blaabjerg has received 17 IEEE Prize Paper Awards, the IEEE Power Electronics Society Distinguished Service Award in 2009, the EPE-PEMC Council Award in 2010, the IEEE William E. Newell Power Electronics Award in 2014, and the Villum Kann Rasmussen Research Award in 2014. He was an Editor-in-Chief of the IEEE Transactions on Power Electronics from 2006 to 2012. He was nominated in 2014 and 2015 by Thomson Reuters to be between the most 250 cited researchers in Engineering in the world.